PAPER

Check for updates

Spermidine carbon dots enhance thermotolerance by modulating photosynthesis and cellular redox homeostasis in tomato†

Min Zhong, [iD] [a] Lingqi Yue,[a] Qingqing Chen,[a] Hui Wang,[a] Bingfu Lei, [iD] [b] Xian Yang[a] and Yunyan Kang*[a]

In this study, we demonstrate and elucidate how spermidine carbon dots (Spd-CDs) enhance tomato tolerance under heat stress (45 °C). Foliar-applied Spd-CDs (6 mg L^{-1}) have a higher maximum quantum efficiency of PSII (45.3%) and net photosynthesis rate (38.6%) compared to after heat stress for 12 hours. Similarly, 6 mg L^{-1} Spd-CDs increased the maximum ribulose-1,5-bisphosphate regeneration rate, maximum ribulose-1,5-bisphosphate carbohydrate/oxygenase carboxylation rate by 10.6% and 41.7%, 33.9% and 82.4%, respectively, accompanied by obvious physiological responses of chloroplast and increased the electron transfer rate (21.3% and 23.1%) were found under normal (25 °C) and high temperature, respectively. Heat stress-induced oxidative stress was significantly alleviated in Spd-CD-treated plants through the lowered accumulation of reactive oxygen species (ROS) (20.7%) and lipid peroxidation (10.9%), along with an elevated ratio of glutathione/oxidized glutathione (GSH/GSSG) (22.6%) and ascorbate acid/dehydroascorbic acid (AsA/DHA) (78.8%), and other antioxidant enzymes, including the ascorbate peroxidase (52.3%), monodehydroascorbate reductase (20.1%), dehydroascorbate reductase (18.3%), glutathione reductase (14.3%), glutathione S-transferase (16.2%), catalase (32.0%), superoxide dismutase (22.9%). Furthermore, using an inhibitor of GSH biosynthesis, buthionine sulfoximine, the Spd-CD induced heat tolerance was compromised, indicating that Spd-CDs induced thermotolerance may be dependent on the AsA–GSH cycle. Taken together, the application of Spd-CDs safeguarded the photosystem complex and ameliorated oxidative damage, thus enhancing thermotolerance. This study put forward that Spd-CDs are a potential tool for plants that are better addressed to the challenges of climate change.

Environmental significance

Carbon dots have demonstrated enormous potential to improve agricultural production. In this study, we found six mg L^{-1} of spermidine carbon dots (Spd-CDs) has outstanding effects on promoting photosynthetic capacity and enhance thermotolerance in tomato. This study on the mechanisms of thermotolerance induction by Spd-CDs proves the potential capacity of nano-enabled agriculture to improve photosynthesis with low-dose amendments that simultaneously reduce environmental negative impact. These findings can not only contribute to the sustainable development of agriculture but also to actively address the challenges posed by climate change.

Introduction

It is estimated that approximately 9.6 billion people will need more food by 2050, and feeding them will require agricultural production to increase by 25–70%.[1,2] More worryingly, about 700 million people in the world were hungry in 2020. Meanwhile, the global temperatures will increase by 1 to 4 °C by 2100, which will lead to a remarkable decline in plant growth, these changes are a vital threat to global crop growth and production, especially in subtropical Asia and the tropics.[3,4] Overcoming this situation will need some strategies to maintain high plant productivity for food security at high temperatures.

Photosynthesis, as the cornerstone of plant growth and production, is reasoned to play a crucial role in crop yield. Plant productivity can be dragged down by high temperatures

[a] *College of Horticulture, South China Agricultural University, Guangzhou 510642, P. R. China. E-mail: kangyunyan@scau.edu.cn*

[b] *Key Laboratory for Biobased Materials and Energy of Ministry of Education, Guangdong Provincial Engineering Technology Research Center for Optical Agriculture, College of Materials and Energy, South China Agricultural University, Guangzhou 510642, P. R. China*

This journal is © The Royal Society of Chemistry 2023

Environ. Sci.: Nano, 2023, **10**, 595–610 | 595

by damaging the photosynthesis process as it plays a basic role in the production of biomass. Heat stress decreases the CO_2 assimilation rate (Pn), and increases the accumulation of potent reactive oxygen (ROS) species while the electron-consuming capacity in the Calvin cycle becomes abnormal.[5,6] The ROS accumulation mainly hit the repair function of the PSII system principally targeting to chloroplast structure, and partly to the deactivated Rubisco.[7] As an inescapable result, various kinds of ROS including hydrogen peroxide (H_2O_2), hydroxyl radicals ($O^{\cdot}$), singlet oxygen, and superoxide anions are produced during photosynthesis. Although a series of mechanisms for ROS-balancing have been found to quencher the excess accumulation of ROS in the chloroplast, redox homeostasis is easy to destroy under stress conditions.[8] Antioxidant enzymes, for example, glutathione reductase (GR), monodehydroascorbate reductase (MDHAR), dehydroascorbate reductase (DHAR), and ascorbate peroxidase (APX), superoxide dismutase (SOD), peroxidase (POD), catalase (CAT), and some antioxidant molecules, such as glutathione (GSH) and ascorbic acid (ASA) in the ASA–GSH cycle, are important to address a reasonable ROS level and the balancing of the cell redox.[9]

The time-consuming and laborious characteristics of traditional agricultural practices and breeding programs seem to be unable to effectively manage the heat stress, as the average global temperature is rising by about 0.2 °C per decade and will rise 1.8–4.0 °C by 2100.[10,11] Nanotechnology, as a major innovative technique, has significant effectiveness, and potential in ensuring plant growth under abiotic stresses compared with traditional methods, unfolding a new aspect in agricultural production.[12] Growing shreds of evidence have revealed that nanoparticles show a direct/indirect impact on plant physiological action, thereby effectively regulating plant growth and stress tolerance, including promoting seed germination, enhancing photosynthesis, and antioxidant activity.[13] The nanomaterials of far-red carbon dots (FR-CDs) with high quantum yield, an efficient converter transferring ultraviolet A light to 625–800 nm far-red emission, which can be directly absorbed and utilized by chloroplast; thus, the photosynthetic activity could be enhanced.[14] Recently, our group reported that the application of 1.5 mg mL^{-1} *salvia miltiorrhiza*-CDs promoted ROS-independent Ca^{2+} mobilization dependent mainly on the hydroxyl and carboxyl groups on CDs, thus increasing the production of cyclic nucleotides and improving plants' environmental adaptability in the saline and nutrient-deficient environment conditions.[15] However, the understanding of the interplay between CDs and plants is still at the early stage, and the molecular mechanism of CDs on plants remains unknown.

Polyamines (PAs), as ubiquitous small molecules with two or more primary amine groups, are recognized as plant growth regulators involved in many cellular functions, including regulation of ion channels, receptor-ligand cross-talk, gene transcription, cell growth, and proliferation.[16] Exogenous spermidine (Spd) or overexpression of *S*-adenosylmethionine decarboxylase (SAMDC, an important

rate-limiting enzyme in Spd biosynthesis), increases heat tolerance by enhancing photosynthesis, maintaining plant growth, and alleviating oxidative damage, and have been considered a new biostimulant.[17] However, the high cost and physicochemical instability of PAs may limit their broad application in plant production. Fortunately, because PAs are highly charged, polycations, with high biocompatibility and can form CDs by a simple heating treatment are widely applied in surface modification and were found at millimolar levels in cells.[18] In living bodies, spermidine-carbon dots (Spd-CDs), as an antibacterial agent, can cause damage to the bacterial membrane and improve faster healing, therefore, Spd-CDs are promising candidates for application due to their extensive interactions with macromolecules.[18] Although Spd-CDs have been widely utilized in animal studies, their application has rarely been reported in plant-related fields.

Tomato is a model plant of the *Solanaceae typically*, and also an important vegetable fruit crop cultivated worldwide, and the optimum temperature for tomato growth is 20–25 °C. Temperature above 35 °C negatively affects growth and fruit set, which reduce yield by up to 70%.[19] Recently, several studies on the effects of CDs in plants under abiotic stress have been carried out, however, it is not still clear whether the Spd-CDs regulated positive potential occurs under heat stress. Based on this, there is poor knowledge to inquire about the functions of Spd-CDs in the management of thermotolerance in tomatoes. Herein, the effects of the Spd-CDs on the phenotypic was studied on tomato seedlings under heat stress, including measuring the Fv/Fm, chloroplast structure, and Calvin cycle to investigate the role of Spd-CDs on photosynthesis in plants, the indexes of ASA–GSH cycle to explore the impact of Spd-CDs on cell antioxidant function. To further study the role of GSH in Spd-CDs improving thermotolerance, we manipulated GSH contents by using buthionine sulfoximine (BSO, an inhibitor of GSH biosynthesis). Thus, this work not only illustrates the unique mechanisms preferring the critical function of ASA–GSH in the thermotolerance of Spd-CDs in plants but also offers a cost-effective and eco-friendly case of Spd-CDs contribution of heat tolerance in the application of plant production. To our knowledge, this is the first study to demonstrate that the application of Spd-CDs might be a valid strategy for the enhancement of plant heat tolerance.

Materials and methods

Fabrication of Spd-CDs

Spd-CDs were synthesized by a one-step hydrothermal process. In brief, 2 g of Spd (Sigma-Aldrich, S2501-5G, Burlington, MA, USA) was added to 70 mL of (0.008 mol L^{-1}) sodium citrate (98 at%, Macklin Co.) solution, then treated under ultrasonication for 30 min. The suspension was placed into a Teflon-lined stainless-steel autoclave and heated at 160 °C for 6 h. The cooling mixture was leached with a 0.22 μm filter membrane for 72 h. The small molecules were removed

with a cellulose dialysis bag (100–500 Da), thereby obtaining Spd-CDs.

Plant material, growth condition, and experimental design

Tomato (*Solanum lycopersicum* L. cv Ailsa Craig) was used in this study, germinated seeds were sown in a growth substrate with a mixture of peat (Jiangsu Xingnong Substrate Technology Co., LTD, A-011, Jiangsu, China) and vermiculite (Jiangsu Xingnong Substrate Technology Co., LTD, A-012, Jiangsu, China) (2:1, v:v), the seedlings as the second true leaf fully expanded were transferred into 250 cm^3 plastic pots with the substrate and were watered with half of Hoagland's nutrition solution. The growth conditions were set as follows: 25 °C/20 °C, 14 h/10 h (day/night), 400 μmol m^{-2} s^{-1} photosynthetic photon flux density (PPFD).

About five week-old seedlings were used for high-temperature treatment in artificial plant growth boxes (Ningbo Jiangnan Instrument Factory, Ningbo, China). To determine the suitable Spd-CDs, each tomato seedling was sprayed with different concentrations of Spd-CDs 20 ml, the concentrations were as follows: 2 mg L^{-1}, 4 mg L^{-1}, 6 mg L^{-1}, 8 mg L^{-1}, and 10 mg L^{-1} or distilled water (ddH$_2$O) once per day for three consecutive days, and were then exposed to normal temperature (control, 25 °C) or high temperature (heat, 45 °C). These different concentrations of Spd-CDs were diluted with ddH$_2$O from 20 mg L^{-1} Spd-CDs. After a 12 h period of temperature treatment, the H$_2$O-treated plants showed strikingly lower thermotolerance properties than the different Spd-CDs-concentration-treated plants. High-temperature stress led to a greater increase in EL, MDA, and H$_2$O$_2$. Pn was significantly declined as a result of the high-temperature treatment. These states were ameliorated by applying different doses of Spd-CDs at high temperatures. Furthermore, we found that Spd-CDs application at 6 mg L^{-1} was the best effective in reducing the damage of heat stress, and enhancing thermotolerance. Based on this, 6 mg L^{-1} Spd-CDs were adopted for the rest of the experiments (Fig. S1†). The BSO at 0.5 mM concentration solution was sprayed on the blade surface for 12 h before high-temperature treatment.[20] According to the previously described growth conditions, photoperiod of 14/10 hour (day/night), and PPFD of 400 μmol m^{-2} s^{-1}, except temperature. Three replicates were used for each treatment, and each replicate contained 12 tomato plants.

Thermotolerance and ROS analysis

After 45 °C treatments, the thermotolerance of the plant was assessed by examining malondialdehyde (MDA) contents, relative electrolyte leakage (REL), H$_2$O$_2$, and O$_2^{\cdot-}$ germination.[21] Briefly, 0.3 g of the sample was ground in 2.0 mL of 10% trichloroacetic acid (TCA) and centrifuged at 10 000*g* for 10 min. 1 mL supernatant was added to 2.0 mL of 0.6% thiobarbituric acid (TBA) and boiled in a water bath for 15 min, and the mixture was cooled immediately in an ice bath. The absorbance of the supernatant was measured at

532 nm by subtracting the absorbance at 532 nm of a solution containing plant extract incubated without TBA from an identical solution containing TBA, and the MDA content was estimated after centrifugation at 10 000*g* for 10 min.

The leaves (0.3 g) were washed with deionized water and placed in tubes with 20 ml of deionized water. The tubes were shaken at 24 °C for 2 h and the electrical conductivity of this solution (L1) was measured. Then, the tubes were boiled for 15 min and cooled to room temperature to measure conductivity a second time (L2). The relative electrolyte leakage (REL) was calculated as follows: REL (%) = (L1/L2) × 100.

The concentration of H$_2$O$_2$ in leaves was measured by monitoring the absorbance of the titanium-peroxide complex at 415 nm. the absorbance was quantified using a standard curve generated from known concentrations of H$_2$O$_2$.

The leaves (1.0 g) were homogenized in 2 mL of 65 mM potassium phosphate buffer (PPB) (pH 7.8) and centrifuged at 5000*g* for 10 min. The reaction solution contained 0.9 mL of 65 mM PPB (pH 7.8), 0.1 mL of 10 mM hydroxylamine hydrochloride, and 1 mL of the supernatant. After the solution was incubated at 25 °C for 20 min, 17 mM sulfanilic acid, and 7 mM α-naphthylamine were added to the solution. The absorbance was measured at 530 nm. The O$_2^{\cdot-}$ concentration was calculated from a standard curve of NaNO$_2$.

Histochemical staining of H$_2$O$_2$ and O$_2^{\cdot-}$ using 1% (w/v) 3-diaminobenzidine (DAB, pH 3.8) and 2 mM nitroblue tetrazolium (NBT) was performed according to Thordal-Christensen *et al.*[22] and Dunand *et al.*[23] with minor modifications, respectively. In the case of O$_2^{\cdot-}$, leaf samples were vacuum infiltrated directly with 0.1 mg mL^{-1} NBT in 25 mM K-HEPES buffer (pH 7.8) and incubated at 25 °C in the dark for 2 h. In the case of H$_2$O$_2$, leaf samples were vacuum infiltrated with 1 mg mL^{-1} DAB in 50 mM Tris-acetate (pH 3.8) and incubated at 25 °C in dark for 24 h. In both cases, samples were rinsed in 80% (v/v) ethanol for 10 min at 70 °C, mounted in lactic acid/phenol/water (1:1:1; v/v), and photographed.

Transmission electron microscopy

Transmission electron microscopy was performed according to the methods detailed by Zhong *et al.*[24] with a few modifications. Tomato leaves were fixed with 2.5% glutaradehyde, then were post-fixed with 1.5% OsO$_4$ for 90 min. The samples were embedded in the Durcupan ACM after dehydrating and were cut using an ultramicrotome. The sections were examined using an H7650 transmission electron microscope (Hitachi, Tokyo, Japan). The parameters of the chloroplast ultrastructure were analyzed using Digimizer software (version 4.1.1.0).

Photosynthetic parameter measurement

The seedlings were adapted about 30 min under dark to estimate the following photosynthetic attributes: maximum

This journal is © The Royal Society of Chemistry 2023

Environ. Sci.: Nano, 2023, **10**, 595–610 | 597

quantum yield of photosystem II photochemistry (Fv/Fm), the quantum yield of PSII [Y(II)], the quantum yield of regulated energy dissipation [Y(NPQ)], the quantum yield of nonregulated energy dissipation [Y(NO)], photochemical fluorescence quenching (q_P), apparent photosynthetic electron transport rate (ETR), and images were also taken by using the Imaging-PAM system (MAXI, Heinz Walz, Effeltrich, Germany).

The Pn was measured using the photosynthesis analyzer system (LI-6800, Li-Cor Inc., Lincoln, NE, America), with PPFD, CO_2 concentration, leaf temperature was set as 200 μmol m^{-2} s^{-1}, 400 μmol mol^{-1}, 25 °C, leaf to air vapor pressure deficit was around 1.0 kPa, and air flow rate through the system was 500 μmol s^{-1}.

The PPFD was set as 1800 μmol m^{-2} s^{-1}, and the stepwise CO_2 concentrations were 50, 100, 200, 300, 400, 600, 800, 1000, 1200, 1500, and 2000 μmol mol^{-1} for the A/Ci response curve. The temperature, relative humidity, and CO_2 contents in the chamber were set to 25 °C, 75%, and 400 ppm before starting measurement, respectively.[25] The maximum rates of Rubisco ($V_{c,max}$) and RuBP regeneration (J_{max}) were measured as described by Ethier and Livingston.[26]

RuBisCO, RuBisCO activase (RCA), and fructose-1, 6-bisphosphatase (FBPase) activity determination

The activity of RuBisCO was examined according to the Ward and Keys' method with slight modification.[27] The tomato leaf samples were ground with extraction buffer (pH 8.0, 2%, 1 mM, 50 mM, 10 mM, 10 mM, insoluble PVPP, EDTA, HEPES, MgCl$_2$, β-mercaptoethanol, respectively), and then the supernatant was obtained by centrifugation at 12000 g for 15 min, all operations were performed at 4 °C. The crude extract was used to assay the total activity. After activating in an activation mixture solution (100 μl) for 15 min at 28 °C, the activity of the initial RuBisCO was evaluated in the reaction medium (100 μl), then the difference in absorbance was measured within 90 s at 340 nm. The activity of RCA was determined using a RuBisCO activase assay kit (Genmed Scientifics, USA). The total FBPase activity and FBPase activity were determined using the crude extract, which was activated in a 100 μl activation mixture reaction (0.1 M, 2 mM, 100 mM, 10 mM, Tris-HCl (pH 8.0), fructose-1,6-bisphosphate (FBP), DTT, MgCl$_2$, respectively). The initial activity was evaluated immediately after homogenization and the enzyme extract was added to start the reaction.[28,29]

Glutathione and ascorbate content assay

For the determination of the levels of glutathione and ascorbate, samples were ground with extraction buffer (2 mL, 6% metaphosphoric acid), and the supernatant was obtained by centrifuging at 12 000g for 10 min at 4 °C to further analysis. To determine the GSH content, the supernatant (10 μL) was mixed with 1.1 mL of the reaction mixture containing 54.5 mM PPB (pH = 7.0) and 0.14% 5,5′-dithio-bis(2-nitrobenzoic acid) (DTNB) (98 at%, Macklin Co,

D806870). After adding GR (Sigma, Santa Clara, CA, USA) to initiate the reaction, the reaction mixture was incubated at 28 °C for 5 min. The GSH content was measured by reading the absorbance of the mixture at 412 nm. The content of GSH was calculated using a standard curve of GSH. The supernatant (10 μL) was mixed with 1.1 mL of the reaction mixture containing 54.5 mM sodium phosphate buffer (pH = 7.0) and 0.14% DTNB, 0.18% nicotinamide adenine dinucleotide phosphate (NADPH) (96 at.%, Macklin Co, N884980) and 0.09 unit GR. The reaction mixture was incubated at room temperature for 30 min and the absorbance was measured at 412 nm for the determination of the total glutathione (GSH + GSSG) content. The GSSG content was calculated according to the differential between total glutathione (GSH + GSSG) and GSH content. To assay the total levels of ascorbate, the supernatant (20 μl) was transferred to a new tube containing PPB (pH 7.4, 0.5 M), and the same amount of dithiothreitol (DTT, 5 mM, Macklin Co, D917653) was added to the supernatant, and then incubated (37 °C, 20 min). N-Ethylmaleimide (NEM, 10 μl, 0.5% w/v) (98 at.%, Macklin Co, N808609) was added to clear the excess DTT. The color reagent (80 μl) (see below) was added to the mixture and incubated. The absorbance was measured at 525 nm. To evaluate the AsA content, the PPB (20 μl, 0.4 M, pH 7.4) was replaced with the DTT and NEM and the procedure was according to the total ascorbate assay. The color reagent was prepared as follows: solution A: orthophosphoric acid, iron chloride (FeCl$_3$) (99 at%, Macklin Co, I809489), TCA (99 at%, Macklin Co, T818878) (31%, 0.6% (w/v), 4.6% (w/v), respectively); solution B: 2,2-dipyridyl (4%) (99 at%, Macklin Co, D806982).[29]

Antioxidant enzyme activity assays

Samples were snap frozen in liquid N$_2$ and extracted using ice-cold phosphate buffer (50 mM, 2% (w/v) PVPP, and 0.2 mM EDTA, pH 7.8). The supernatant obtained after post-centrifugation was used for the evaluation of enzyme activity. The SOD, CAT, APX, MDAR, and DHAR activities were measured. SOD activity was measured at 560 nm by measuring the ability to inhibit the photochemical reduction of NBT, CAT activity was measured at 240 nm following the decomposition of hydrogen peroxide, APX and DHAR activities were measured by a decrease at 290 nm, and an increase at 265 nm, MDAR activity was measured using 1 unit ascorbate oxidase, and the oxidation rate of NADH was followed at 340 nm, GR activity was calculated from the rate of decrease in the absorbance of NADPH at 340 nm, DHAR activity was measured by the increase in absorbance at 295 nm as GSH-dependent production of ascorbate, as previously described.[21,30]

Glutathione S-transferase (GST) activity was examined using the GST detection kit (Solarbio Life Science, Beijing, China) according to the instructions. 0.1 g of the sample was ground with extraction buffer (1 ml) and homogenized by centrifugation (8000 × g, 10 min, 4 °C), the supernatant was

598 | Environ. Sci.: Nano, 2023, 10, 595–610

This journal is © The Royal Society of Chemistry 2023

used for the evaluation of enzyme activity, and was calculated by measuring the change in absorbance at 340 nm.

The content of protein was examined using a BCA protein assay kit (Pierce). All spectrophotometric analyses were performed using a Shimadzu UV-2410PC spectrophotometer (Shimadzu Co., Tokyo, Japan).

RNA isolation and RT-qPCR analysis

Total RNA was isolated from the samples as previously described.[23] To assay the concentration of RNA, a Nano-300 spectrophotometer was used (Allsheng, Hangzhou, China). DNase I was used for removing genomic DNA contaminants, 1 µg total RNA was used to synthesize cDNA using a HiScript II 1st Strand cDNA synthesis kit (Vazyme Biotech, Nanjing, China, cat. No. R212). The SYBR Green PCR Master Mix was used for RT-qPCR (TransGen Biotech, Beijing, China, cat. No. AQ131) on an ABI ViiA7 real-time PCR system (Applied Biosystems, CA, USA). The RT-qPCR primers are listed in Table S1.† *Actin* was used as a control. Each experiment consisted of at least three biological repetitions. The relative expression levels for each gene expression were calculated according to the methods of Livak and Schmittgen (2001).[31]

Statistics

The data were statistically analyzed using the SPSS 20 statistical software (IBM SPSS statistics 20, NY, U.S.A). The experimental data were categorized according to Duncan's multiple range test at $P < 0.05$. The values in the figures and tables are the mean standard deviation (SD) (at least $n = 3$).

Results and discussion

Physicochemical properties of Spd-derived CDs

The Spd-CDs are nanodots of 1.4 nm (Fig. 1A and B) in size as measured by TEM, which are easily dissolved in water. Fourier transform infrared (FTIR) spectroscopy showed that the broad absorption band at 3200–3600 cm^{-1} attributed to the stretching vibration of O–H and N–H, suggesting the presence of phenolic hydroxyl group and carboxylic acids. The peaks at 1706 and 1632 cm^{-1} can be ascribed to the C=O stretching vibration of carboxylic acids and aromatic ketone. The peak at 1400 cm^{-1} indicates the presence of a bending vibration of –OH. The band at 1220 cm^{-1} is attributed to the stretching and bending vibrations of C–O (Fig. 1C). The XPS survey spectrum showed that the Spd-CDs are composed of C, N, and O elements with atomic ratios of 67.35%, 6.7%, and 25.94%, respectively. FT-IR spectrum, C1s, O1s, and N1s XPS spectra show that the main groups of Spd-CDs are carboxyl, hydroxyl carbonyl, and ether bonds (Fig. 1D, F, G, and H). These results show that the surface of the prepared Spd-CDs is rich in N–(C)$_3$, C–C, C–O, C=C, and C=O.

Spd-CDs enhance thermotolerance in tomato seedlings

Firstly, to evaluate the thermotolerance role of Spd-CDs in tomatoes, we evaluated the effects of different concentrations of Spd-CDs on the mitigation of heat stress in tomato plants. As shown in Fig. S1,† 6 mg L^{-1} Spd-CDs was chosen as the optimal dose for further experiments as it can dramatically reduce the inhibition effect of heat stress, compared with the non-stressed controls, on EL (3.9- and 1.1-fold, respectively), Pn (−65.6% *vs.* −38.1%), MDA (0.86- and 0.28-fold,
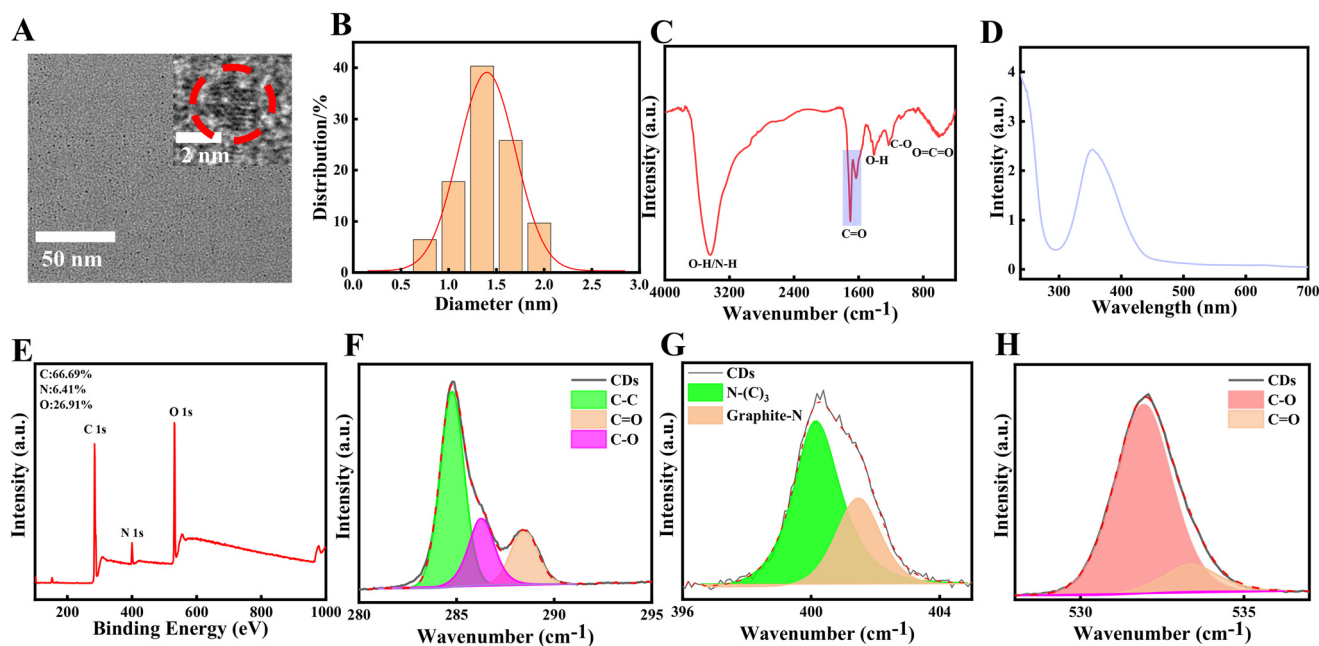

Fig. 1 TEM and HRTEM photos (A), size distribution (B), FTIR spectrum (C), UV-vis absorption spectrum (D), XPS survey spectrum (E), C1s spectrum (F), N1s spectrum (G), O1s spectrum (H). The size distribution in (B) is calculated randomly from (A).

This journal is © The Royal Society of Chemistry 2023

Environ. Sci.: Nano, 2023, **10**, 595–610 | **599**

respectively), H_2O_2 (0.69- and 0.04- fold, respectively), and the degree of wilting in H_2O-treated plants was more severe than that of 6 mg L^{-1} Spd-CDs after 24 hours of the high-temperature treatment (Fig. 2A). These results suggest that Spd-CDs can exert positive thermotolerance effects in tomato plants.

High temperatures damage the photosynthesis process, which triggers a series of influx that regulates downstream heat stress response, and also impairs other cell functions.[32,33] The Fv/Fm, as an important chlorophyll fluorescence indicator, is frequently used to assay photosynthetic performance.[34] The values of Fv/Fm are decreased when plants are subjected to various stresses, and the application of CDs highlights a positive role as a regulator of photosynthetic performance.[35,36] Exogenous CDs induce enhancement of photosynthesis by increasing

electron transport *in vivo*.[37] It was reported that saline-alkali stress was mitigated by the application of CDs by up-regulating the photosynthesis efficiency and improving tomato growth.[38] Thus, the gathered evidence indicates that CDs play a crucial role in the protection of photosynthesis under abiotic stress. In this study, we showed that Spd-CDs maintained better plant growth in tomatoes were exposed to high temperatures (Fig. 2A). As expected, Spd-CDs enhanced the value of Fv/Fm (45.3%) in tomato seedling leaves under heat stress (Fig. 2B and C). It may be that Spd-CDs effectively deal with too much light energy to trigger plant photoprotective mechanisms. Furthermore, the decrease in EL (38.9%), increase in the Pn (38.6%), and the relative water content (18.3%) levels, as important parameters of plant health, consistent with the physiological index in Spd-CDs-pretreated in tomato plants under heat stress (Fig. 2D–F).
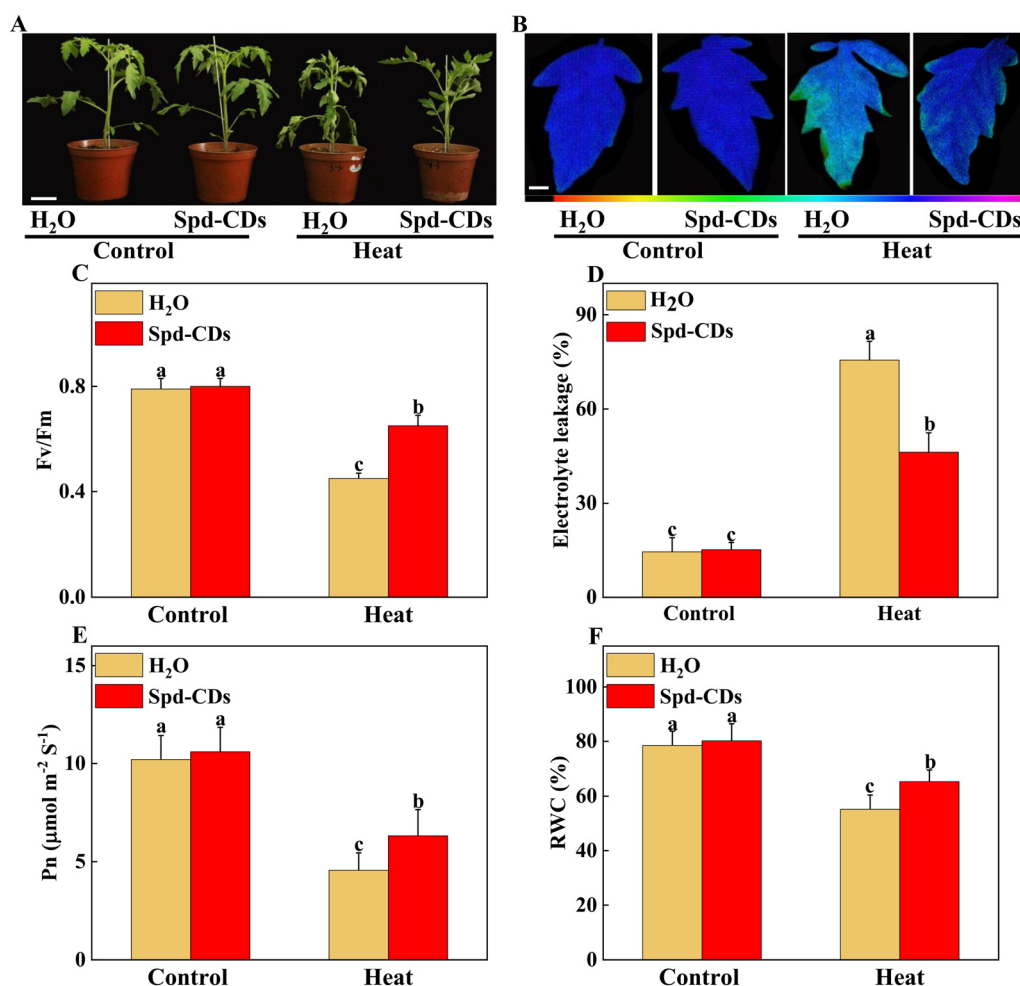

Fig. 2 Phenotypic and physiological analysis of Spd-CDs on the enhancement of thermotolerance in tomato plants. The phenotypes of H_2O, exogenous Spd-CD-pretreated plants under normal temperature (25 °C) or high temperature (45 °C) treatment, and the plant images was taken in 24 h later, bar = 10 cm (A); The pseudo-color images showing the maximum quantum efficiency of PSII (Fv/Fm), bar = 1 cm, the color code in the images ranges from 0 (black) to 1.0 (purple) (B), and the values of Fv/Fm in the terminal leaflets of the fourth leaves under different temperature treatments (C); the relative electrolyte leakage (D), the net photosynthesis rate (Pn) (E) and leaf relative water content (F) of tomato leaves after 12 h of different temperature treatments. The Pn values were measured under photosynthetically active radiation (PAR) at 800 μmol m^{-2} s^{-1}. Images shown in a and B were digitally extracted and scaled for comparison. The data in C to F are presented as mean values ± SD; $n = 3$. Different letters indicate significant differences between treatments ($P < 0.05$, Duncan's multiple range test). Three independent experiments were performed with similar results.
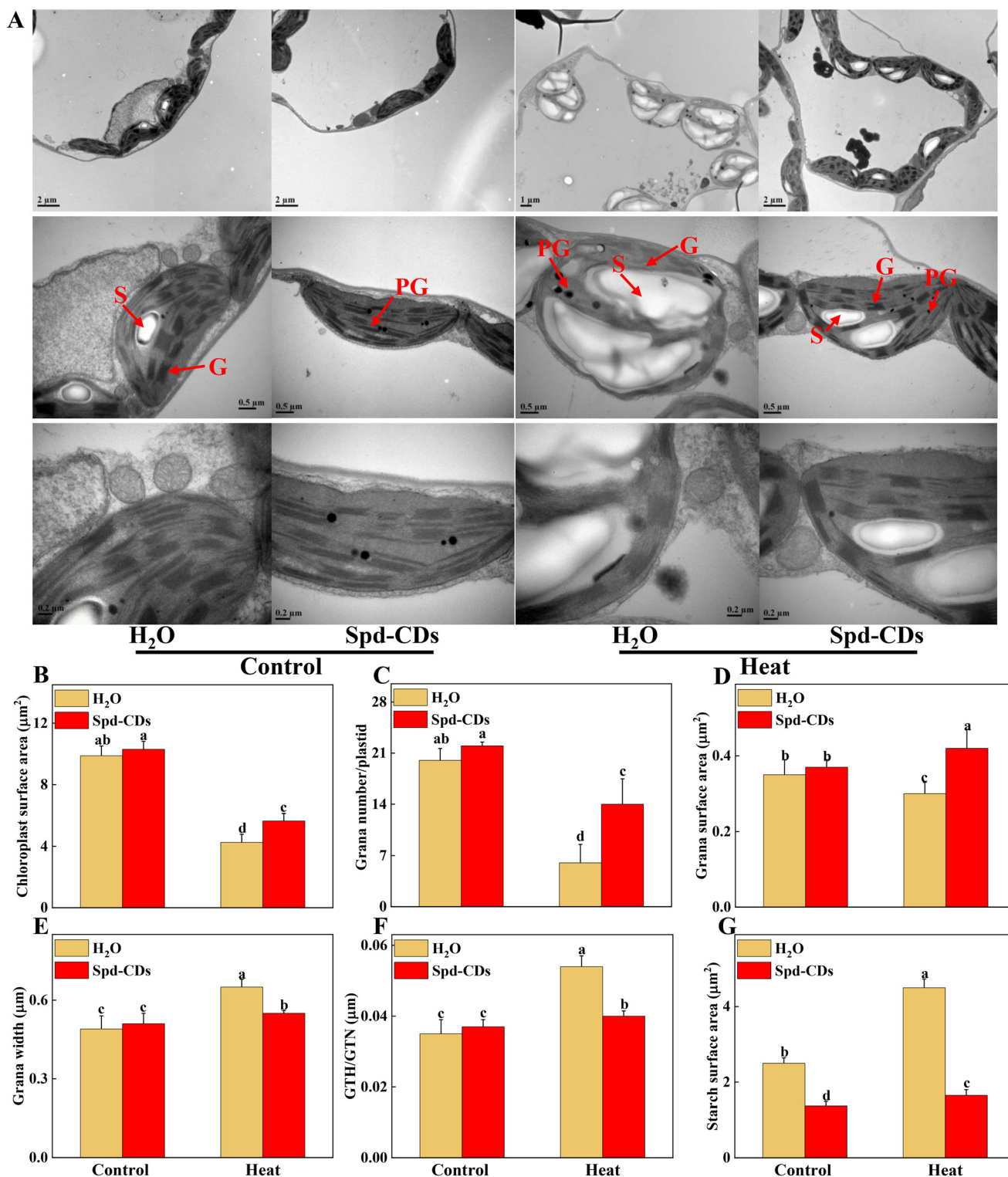
Fig. 3 Transmission electron microscopic (TEM) micrographs of cell ultrastructure in upper leaves of tomato plant. The effects of Spd-CDs on the ultrastructure of chloroplast after 24 h under normal temperature (25 °C) or high temperature (45 °C) treatment, G, granum thylakoid, PG, plastoglobule, S, starch (A). The surface area of chloroplast (B), grana number per plastid (C), grana surface area (D), grana width (E), GTH/GTN (F), and starch surface area (G) under different temperature treatments. The data in B to G are presented as mean values ± SD; n = 10. Different letters indicate significant differences between treatments (P < 0.05, Duncan's multiple range test). Three independent experiments were performed with similar results.

Collectively, these results showed that Spd-CDs play an important role in plant heat tolerance.

Spd-CDs involved in chloroplast development and CO_2 assimilation

The function and structure of chloroplasts with decreased photosynthesis were disrupted by ROS over-production at high temperatures.[39] This process was effectively and clearly examined by the TEM technique. In this study, TEM results showed that Spd-CDs displayed less damage on the ultrastructure of the chloroplast compared to high-temperature exposition treatment. In heat stress, a large number of thylakoids were entirely or partly ruptured or destroyed accompanied by starch grains and grana stacks became bigger (1.8- and 1.3-fold, respectively), but the application of Spd-CDs maintained the integrity of thylakoid, the morphology of chloroplast had no change, a few thylakoids were partly swollen with little accumulation of starch grains. Meanwhile, the membranes of thylakoid and chloroplast were more cheapened and granum thylakoids were more piled shapely in the Spd-CD-treated than H_2O-treated plants under heat stress (Fig. 3). Subsequently, the morphometric analysis was performed based on the schematic illumination of the chloroplast ultrastructure (Fig. S2†). Spd-CDs retained a 32.9% larger surface area of chloroplast, 133.3% more number of grana in the chloroplast, and 40.0% bigger surface area of grana compared with those of H_2O-treated plants under heat stress, while the plastoglobuli were significantly decreased in Spd-CD plants than that in the H_2O-treated plants under normal and heat conditions. Additionally, the chloroplast ultrastructure did not show any noticeably significant difference, but the cell wall thickness was significantly increased (112.3%) in all Spd-CD-treated plants under normal temperature (Fig. S3†). Recent reports revealed that FR-CDs or Spd is involved in the formation of PSII in plants,[14,40] stated that the development of chloroplast grana in Spd-CD plants. Also, the levels of the transcript abundance were significantly decreased under high temperatures, such as *PSI*, *PSII*, *LCHI*, *LHCII*, and *PET*, which are associated with electron transport, light harvesting, and carbon dioxide assimilation, obviously the downregulation of these gene abundances was higher in only heat stressed seedlings than in Spd-CD-treated plants, were also impacted by Spd-CDs under normal conditions, which were consistent with the ultrastructure of chloroplast (Fig. 3 and S4†). The total protein content of heat-stress plants was also remarkably lower (−37.9%) than those in Spd-CD plants under high-temperature stress treatment (Fig. S5†). Generally, the transcript of LHC proteins was higher, and the thylakoid membrane was less degraded in Spd-CD-treated plants than in H_2O plants under heat stress. Importantly, the accumulation of starch in leaves could enhance reactive carbonyls, and the photosynthesis rate is downregulated in plants exposed to heat stress.[41] In addition to the scavenging

system of starch-induced reactive carbonyls, the observed increase in cell-wall thickness could be another mechanism to avoid heat conditions in Spd-CD-treated plants (Fig. 3G and S3†). Taken together, our results indicate that Spd-CDs affect chloroplast development, which were critical to minimize the damage to the photosystem and reduce oxidative stress under harsh conditions.

The energy of light absorbed by PSII antennae in plants can be utilized by photochemistry or dissipated, meanwhile, the PSII also acts as the major ROS generation site in the chloroplast. Abiotic stresses (*e.g.* high or low-temperature stress) can influence energy allocation in the apparatus of the photosystem.[42,43] Reasonable distribution of light energy in the photosynthetic apparatus by different lines in complexes of PSII is a crucial response to environmental factors.[44,45] The Spd-CDs and H_2O-treated plants had similar levels of Fv/Fm, as well as the values of Φ_{PSII}, $Y(II)$, $Y(NO)$, $Y(NPQ)$, q_P, and ETR under normal conditions. Interestingly, the ETR was significantly higher (95.5%) in Spd-CD-treated plants than those of controls under no-stress conditions, indicating that Spd-CDs enhanced the real efficiency of PSII although their full PSII's potential was not significant. This difference could be as Spd-CDs increased chloroplast surface area and Pn, which led to absorbing more light energy (Fig. 2 and 4). When plants were exposed to high temperatures, significant reductions of the Φ_{PSII} (33.7%), $Y(II)$ (29.8%), q_P (28.6%), and ETR (23.1%) values were observed in the H_2O-treated plants, compared to those in Spd-CD plants, which became disruptive to the PSII function. Yet, the trend of the yield for other energy losses with the accumulation of $Y(NO)$ (16.0%) and $Y(NPQ)$ (10.9%) was significantly increased in H_2O-treated plants, but heat stress-induced elevation was significantly reduced after the application of Spd-CDs, indicating that the plants treated with Spd-CDs were absorbing excessive light energy and positively scattering excess energy as a mechanism against heat stress. Thus, Spd-CDs balance the absorption and utilization of light energy and increase low ROS accumulation of components while showing strong PSII actively in the chloroplast under heat stress, subsequently increasing the thermotolerance.

Various studies have proved that Rubisco activase in the Calvin cycle is an interesting target area for enhancing photosynthesis under heat stress.[46,47] Thus, keeping Rubisco activation is crucial for increasing the thermolability of plants. In addition, recent work demonstrated that increasing both Rubisco and Rubisco activase could result in an enhancement of CO_2 assimilation under normal temperature conditions.[48] Here, under the normal temperature, the J_{max} and $V_{c,max}$ did show significant differences between the control and Spd-CD-treated plants. At 45 °C, J_{max} was higher (27%), and $V_{c,max}$ was higher (45%) in Spd-CD-treated plants than in H_2O-treated plants. On the other hand, under normal conditions, the initial Rubisco activity and Rubisco activase state were not significantly different between control and Spd-CD treatment, except the Rubisco activase and initial FBPase activity, and they were remarkably higher, 13.3% and
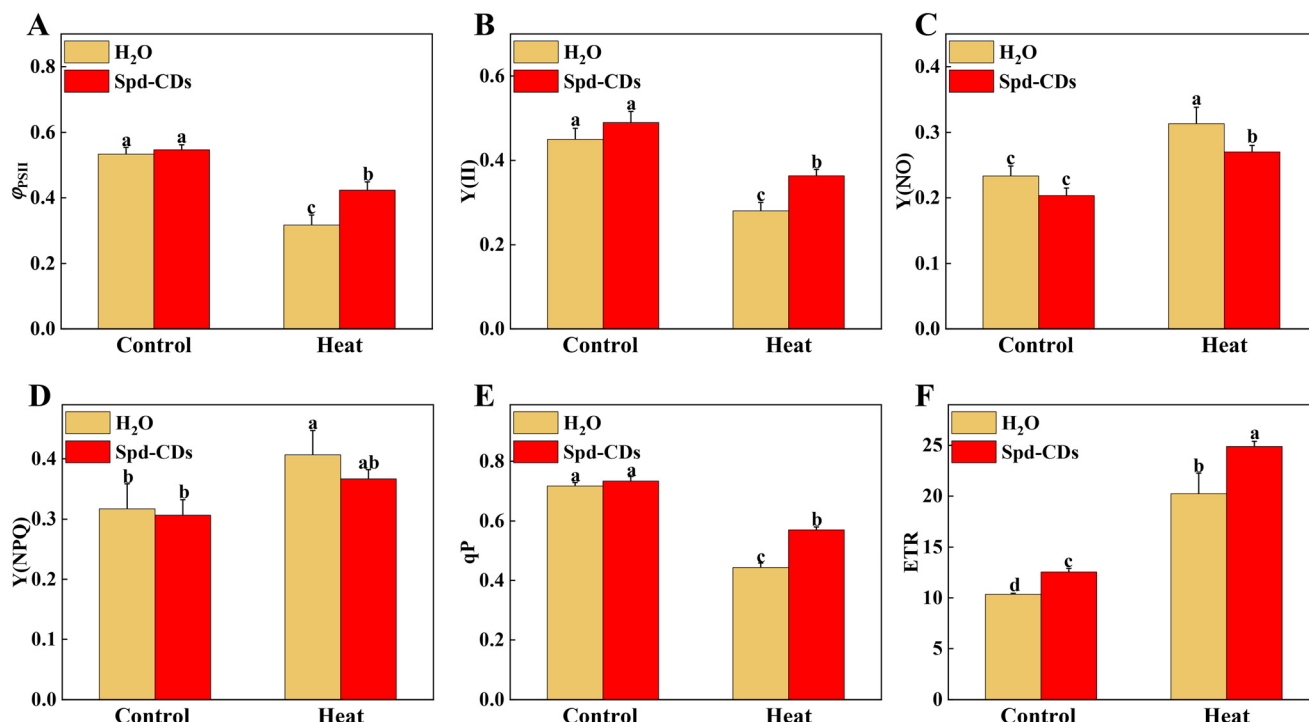
602 | *Environ. Sci.: Nano*, 2023, **10**, 595–610

This journal is © The Royal Society of Chemistry 2023

Fig. 4 Chl fluorescence analysis in Spd-CD pretreated plants under normal temperature (25 °C) or high temperature (45 °C) treatment. (A) Φ_{PSII}, (B) $Y(II)$, (C) $Y(NO)$, (D) $Y(NPQ)$, (E) q_P, (F) ETR. The data are presented as mean values ± SD; $n = 3$. Different letters indicate significant differences between treatments ($P < 0.05$, Duncan's multiple range test). Three independent experiments were performed with similar results.
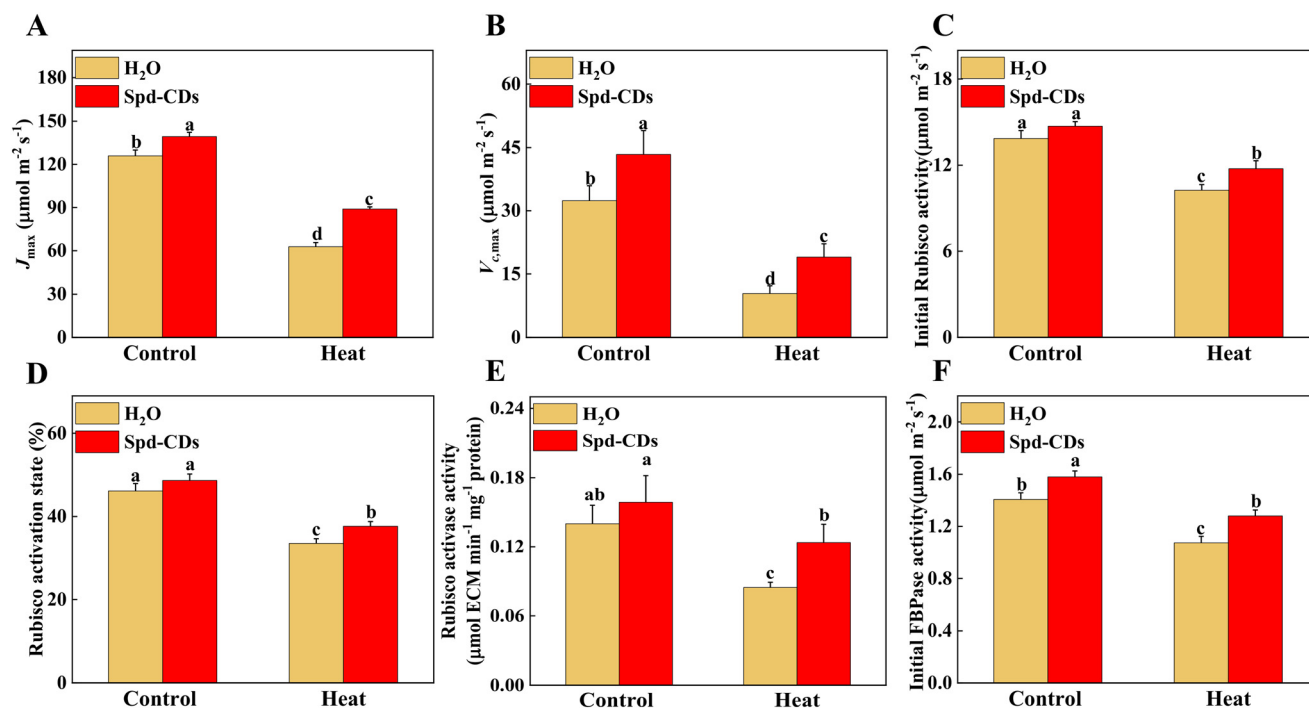

Fig. 5 Photosynthetic parameters analysis in Spd-CD pretreated plants under normal temperature (25 °C) or high temperature (45 °C) treatment. Maximum ribulose-1,5-bisphosphate (RuBP) regeneration rate (J_{max}) (A), maximum ribulose-1,5-bisphosphate carbohydrate/oxygenase (Rubisco) carboxylation rate ($V_{c,max}$) (B), the initial carboxylation activity of Rubisco (C), the activation state of Rubisco (D), the activity of Rubisco activase (E), the initial activity of fructose-1,6-bisphosphatase (F). The data are presented as mean values ± SD; $n = 3$. Different letters indicate significant differences between treatments ($P < 0.05$, Duncan's multiple range test). Three independent experiments were performed with similar results.

This journal is © The Royal Society of Chemistry 2023

Environ. Sci.: Nano, 2023, **10**, 595–610 | **603**

12.3%, respectively, than in H_2O-treated plants. At high temperatures, these activities were significantly higher in Spd-CD plants than in H_2O-treated plants. The results showed that Spd-CDs induced a higher Rubisco activase, along with higher levels of Rubisco content, initial Rubisco activity, and an increase in $V_{c,max}$ (Fig. 5). Similarly, the expression of Calvin cycle-related genes, such as *FBAs*, *PGKs*, *SBPase*, *RCAs*, and *FBPs*, that were induced by Spd-CDs, were down-regulated by heat treatment, and heat-induced decline in the transcripts of genes was more severe than in Spd-CD-treated plants, accompanied by an increase in Pn at high temperature than that in the heat treatment alone, implying that Spd-CDs not only enhanced photosynthetic capacity under normal conditions but also help plants to safeguard the Calvin-cycle by inducing the transcript levels of

corresponding genes and enzyme activities when faced with high temperature (Fig. S6† and 2). The RuBP regeneration has two faces on the electron transport chain and the Rubisco enzyme in photosynthesis.[49] The expression and initial activity of FBPase were increased in the Spd-CD-treated plants, and the J_{max} was also affected under normal or heat conditions. Thus, these results clearly show that the Spd-CDs could regulate the Calvin cycle to improve the heat tolerance of tomato seedlings.

Spd-CDs inhibit over-accumulation of ROS by regulating the ASA–GSH cycle to enhance thermotolerance

Probably, we have provided the first evidence of the effective role of Spd-CDs on the PSII-ROS module in increasing
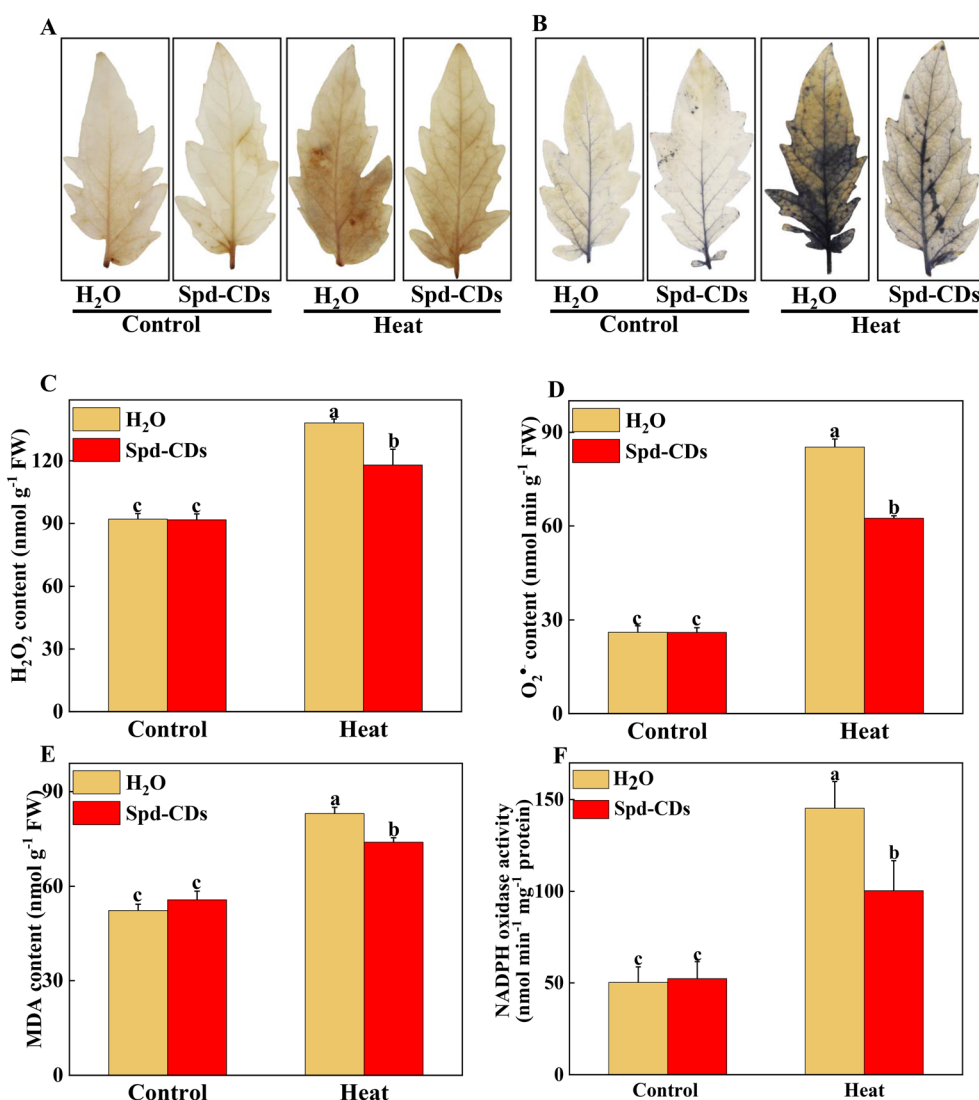

Fig. 6 Response of ROS accumulation in Spd-CD pretreated plants under normal temperature (25 °C) or high temperature (45 °C) treatment. Representative images of H_2O_2 accumulation as observed by DAB staining (A). Representative images of $O_2^{\cdot-}$ accumulation as observed by NBT staining (B). Quantification of H_2O_2 and $O_2^{\cdot-}$ (C and D), MDA content (E), NADPH oxidase activity (F). The data are presented as mean values ± SD; $n = 3$. Different letters indicate significant differences between treatments ($P < 0.05$, Duncan's multiple range test). Three independent experiments were performed with similar results.

604 | *Environ. Sci.: Nano*, 2023, **10**, 595–610

This journal is © The Royal Society of Chemistry 2023

thermostability in tomato plants. Briefly, the antioxidant enzyme activities were significantly reduced, but the levels of H_2O_2 and O_2^- accumulation increased remarkably in heat-stressed seedlings (0.5- and 2.3- fold, respectively). Similarly, DAB and NBT staining showed that heat-treated leaves had a more vigorous intensity of brown precipitation and blue spots than those of the Spd-CD-treated ones, and there was

no significant difference observed between the control and Spd-CD treatment under normal conditions (Fig. 6A and B). The levels of H_2O_2 and O_2^- had 14.6% and 26.7% lower accumulations in the Spd-CD-treated plants than in the heat-treated ones, which is consistent with the histochemical straining results and the MDA content (Fig. 6C–E). Furthermore, the NADPH oxidase activity was deepened
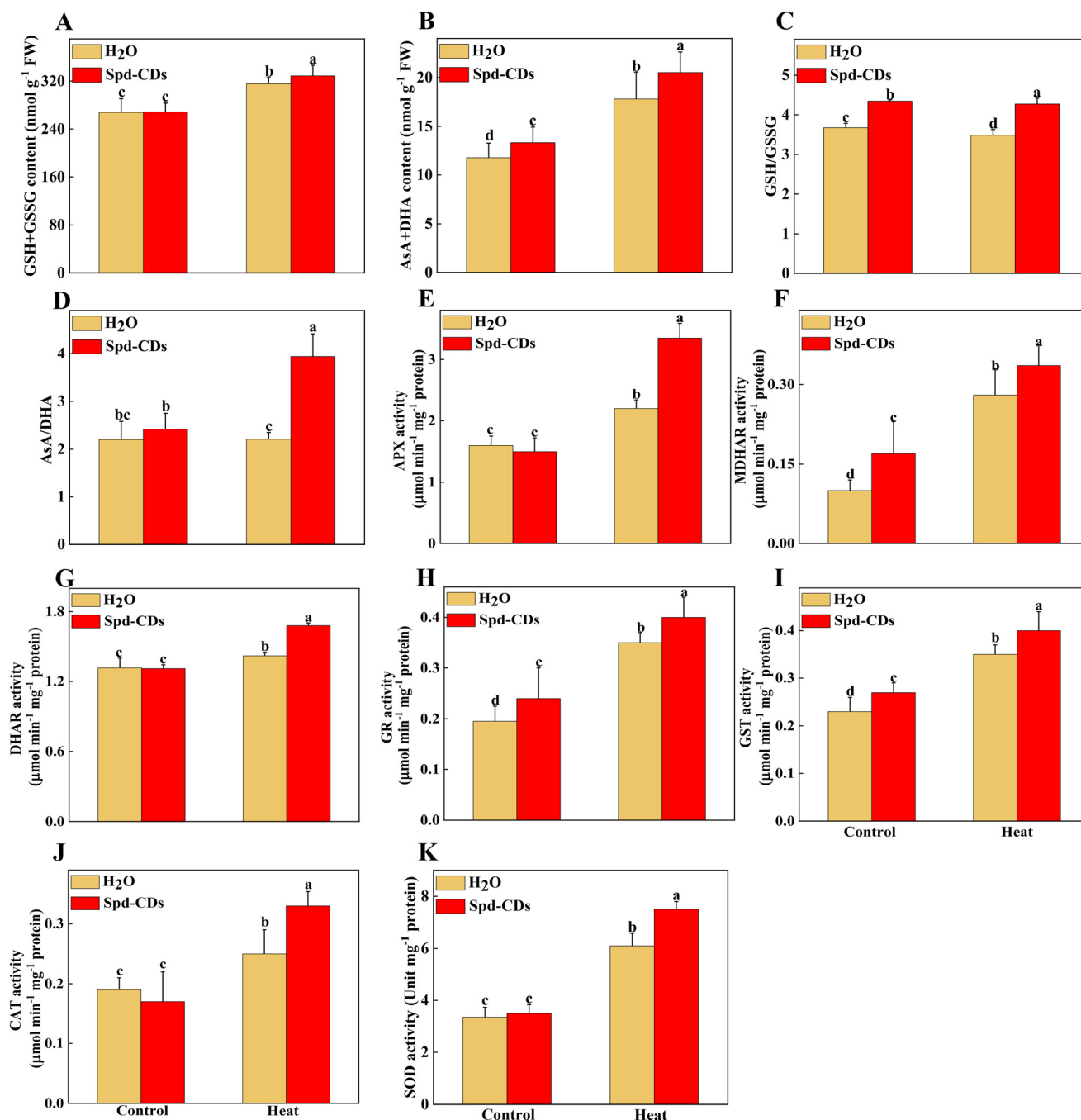

Fig. 7 Antioxidants and enzyme activities in Spd-CD pretreated plants under normal temperature (25 °C) or high temperature (45 °C) treatment. The effects of Spd-CDs on antioxidants (GSH + GSSG content, AsA + DHA content, GSH/GSSG and AsA/DHA ratio) in response to high temperature (A–D). The effects of Spd-CDs on enzyme activities (APX, ascorbate peroxidase; MDHAR, monodehydroascorbate reductase; DHAR, dehydroascorbate reductase; GR, glutathione reductase; GST, glutathione S-transferase activity; CAT, catalase; SOD, superoxide dismutase;) in response to high temperature (E–K). The data are presented as mean values ± SD; n = 3. Different letters indicate significant differences between treatments (P < 0.05, Duncan's multiple range test). Three independent experiments were performed with similar results.

This journal is © The Royal Society of Chemistry 2023

Environ. Sci.: Nano, 2023, **10**, 595–610 | **605**

about 3 times compared with the control under high-temperature conditions, and its activity was alleviated after the application of Spd-CDs (Fig. 6F). This clearly shows that tomato seedlings treated with the Spd-CDs accumulated lower ROS than that in the heat-treated plants. Similar results were reported for *Salvia Miltiorrhiza*-derived carbon dots in Italian lettuce seedlings under salt stress.[50] Meanwhile, the expression levels of *DHAR, MDHAR, APX, CAT, SOD GPX*, and *GR* in Spd-CD-treated seedlings were higher than those under only heat stress conditions. Furthermore, the Spd-CD-treated seedlings showed lower ROS accumulation and expression levels of ROS-related genes (*Rbohs*), but the opposite trends were found in the heat-stress-treated seedlings (Fig. 6 and S8†). These results indicate that Spd-CDs could play a crucial role in mediating ROS accumulation. Additionally, Spd-CDs could be absorbed onto the surface of leaves, which act as removers of free radicals, directly clearing excess ROS. Notably, this fine mechanism of Spd-CDs directly mediating ROS balance needs to be further demonstrated by more evidence from experiments.

The antioxidant enzymes are involved in the equilibrium of the cellular redox status, which controls normal ROS levels in cells to ensure healthy plant growth.[6] Similarly, the GSH and DHA contents of the leaves of Spd-CD-treated plants exhibited a similar trend compared with those of the control treatment under normal conditions (Fig. S7†), but their contents were changed in the Spd-CD-treated plants under heat stress. Specifically, the content of GSH in Spd-CD-treated plants was higher than that in the control treatment under heat stress, reaching around 1.2 times higher than that of the control group. Inversely, the DHA content of leaves in the Spd-CD-treated group was significantly lower by 25.4% than that of the control group under heat stress. Similarly, the upregulated GSSG content induced by heat was significantly reduced by 11.4% after the application of Spd-CDs, and it was worth mentioning that the GSSG content in the Spd-CD treatment even showed the lowest level under normal conditions (Fig. S7†). Further analysis showed that the GSH + GSSG and AsA + DHA contents, the AsA/DHA, and GSH/GSSG ratios under Spd-CD treatment were higher than that of the control groups under heat stress. Moreover, these ratios were also even more significant between the Spd-CD treatment and control group under normal conditions (Fig. 7A–D). Subsequently, the enzymatic activity of the AsA–GSH cycle, APX, MDHAR, DHAR, GR, and GST, were also examined as indicators of the antioxidant status of this cycle. As shown in Fig. 7E–I, the activities of MDHAR, GR, and GST were markedly induced by 70.0%, 23.1%, and 17.4% under Spd-CD-treatment compared with the control, while there were no significant differences observed for APX, DHAR, CAT, and SOD activity under normal conditions. Notably, heat-induced activities of MDHAR and GR were increased by 20.0% and 14.3% after the addition of Spd-CDs, which is consistent with the activity of APX (increased by 52.3%). Moreover, the activities of GR and GST were obviously increased by 79.5% and 52.2%, respectively, after heat

treatment in comparison to control plants, and further increased by 1.1 and 0.73 times after the application of Spd-CDs (Fig. 7H). Furthermore, antioxidant enzymes play a crucial role in ROS scavenging pathways, the enzymatic activities of three types of ROS-scavenging enzymes (APX, CAT, and SOD) were higher in Spd-CD-applied groups than those of the control group under heat conditions (Fig. 7E, J and K). Overall, the results indicate that Spd-CD-induced heat stress tolerance is largely related to ROS-scavenging capacity. Spd-CD-treated plants had higher enzymatic activities of GR, APX, DHAR, and MDHAR, and higher expression of their encoding genes than those in the H_2O-treated plants under heat stress conditions. Moreover, they are the important constituent enzymes in the ASA–GSH cycle. GR was related to the content of cell GSH.[51] Spd-CDs enhanced the APX activity, which played an important role in ROS scavenging and maintaining a turnover rate of the ASA–GSH cycle.[52] Some MDHA could be changed to ASA or DHA by MDHAR, and DHA can also be transformed into ASA with the participation of DHAR and GSH, ultimately removing excess H_2O_2.[53] After the application of Spd-CDs, the up-regulated GR and MDAR induced the accumulation of GSH and ASA levels, accompanied by ASA/DHA and GSH/GSSH ratio, and resulted in the decline of H_2O_2-induced oxidative stress (Fig. 7). Thus, Spd-CDs mediate oxidative stress by maintaining the activities of related enzymes in the ASA–GSH cycle to balance redox homeostasis.

In addition to the antioxidant enzymes, the AsA–GSH cycle, as a non-enzymatical antioxidants in plants, also plays an important role in maintaining the balance of ROS production and cell redox.[54] AsA and GSH as antioxidants play an excellent role in scavenging ROS, to mediate the components of the cell and alleviate the oxidative damage under various stresses.[51,55] GSH also plays a crucial role in Rubisco activation.[56] The Spd-CDs mediate the activation state of Rubisco, and they may be involved in the changes in glutathione redox status. In this study, Spd-CDs can enhance the levels of GSH and AsA, and decrease the contents of GSSG and DHA, thus increasing AsA/DHA and GSH/GSSH ratio, which reflects that the oxidative state of the cell and Rubisco activities are better than that of heat stress conditions. It has been shown that the inhibition of GSH could reduce heat resistance.[57] Therefore, to further analyze whether Spd-CD-mediated GSH is crucial for thermotolerance, we treated tomato seedlings with 0.5 mM BSO. Under normal conditions, the Fv/Fm value was decreased in the BSO treatment compared with the H_2O treatment, but the adverse effect was partially eliminated by the application of Spd-CDs, and the REL also showed no significant difference between BSO and Spd-CD treatments (Fig. S9†). Furthermore, both the BSO and BSO + Spd-CD-treated plants showed a wilting phenotype after heat stress for 24 hours, which is similar to high temperatures. The wilting was worsened by BSO, while it was slightly in BSO + Spd-CD treated plants compared with H_2O-treated plants. As expected, BSO increased the EL, H_2O_2, and MDA contents, more than the heat treatment alone.

606 | *Environ. Sci.: Nano*, 2023, **10**, 595–610
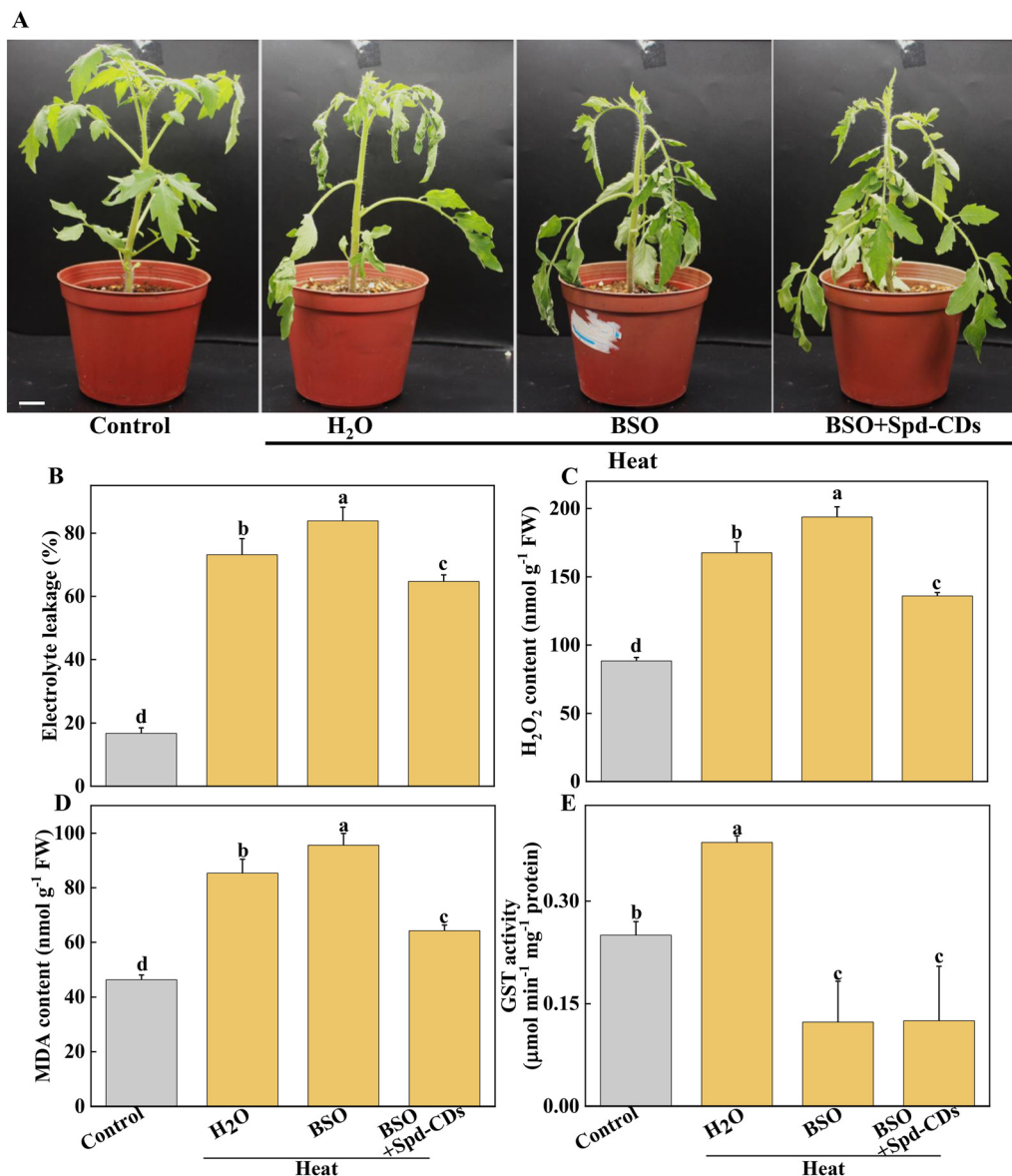
This journal is © The Royal Society of Chemistry 2023

Fig. 8 The effect of Spd-CDs the regulation of thermotolerance of tomato plants under high temperature with or without BSO. The phenotypes of H_2O treated plants under normal temperature, and Spd-CDs with or without BSO under high temperature (45 °C) treatment, the plant images were taken in 24 h later, bar = 10 cm (A). The relative electrolyte leakage (B), the H_2O_2 content (C), MDA content (D) and GST activity (E) of tomato leaves after 12 h of different treatments. The data are presented as mean values ± SD; n = 3. Different letters indicate significant differences between treatments ($P < 0.05$, Duncan's multiple range test). Three independent experiments were performed with similar results.

Importantly, BSO moderately abolished Spd-CD-alleviated heat-induced heat stress (Fig. 8A–C). In addition, the activity of GST increased exponentially with high-temperature treatment, and the application of BSO negatively affected the GST activity in Spd-CD-treated plants, which gave rise to no significant differences in the activity of BSO and Spd-CD-treated plants (Fig. 8D). Briefly, BSO leads to the weakening of heat tolerance, and combined supplementation of Spd-CDs and BSO partially restored the tolerance of heat stress. This further supports that the Spd-CDs were crucial for enhancing high-temperature tolerance by regulating GSH contents. Together with the above results, it can be an assumption that Spd-CDs are efficient at scavenging of ROS

to maintain the normal cellular redox status through the up-regulating in the ASA/DHA and GSH/GSSG ratios, especially under heat stress.

Conclusion

CDs are effective tools for agricultural production and under harsh environmental conditions. Completely understanding the function of CDs in plants is fundamental for their use in agricultural production. In this study, the application of Spd-CDs, synthesized from Spd containing abundant carboxyl and hydroxyl carbonyl groups, can endow redox homeostasis by mediating NADPH-oxidase activity and AsA–GSH cycle that
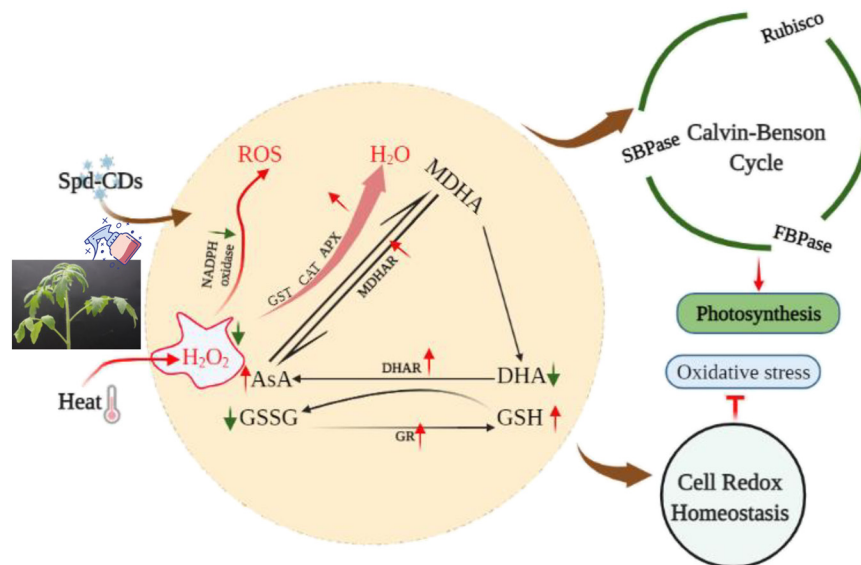
Fig. 9 A proposed model for depicting the role of Spd-CDs in alleviation of heat stress induced the damage in tomato leaves. The arrows exhibit either a decrease (green) or an increase (red) in metabolite concentration or in enzyme activity, respectively.

increases antioxidant enzymes activity, and thus ultimately reduced heat damage in tomato plants. Furthermore, Spd-CDs counteracted the heat stress-induced photosynthetic damage by regulating Calvin-cycles enzyme activity and ROS neutralization. Most importantly, an increase in photosynthetic rate with photosynthetic organ remodeling was achieved by Spd-CDs under normal and heat stress conditions (Fig. 9). Owing to the fact that photosynthesis is the infrastructure in almost all physiological processes in plants, these results elevate the feasibility that Spd-CDs have access to a mediator for enhancing photosynthesis under different environmental conditions. This potential may carry out the environmental or agricultural advantage of Spd-CDs to a certain degree. Collectively, the above results broadly indicated that Spd-CDs could be used as a useful tool to mitigate abiotic stresses, especially in heat stress, which could have advantages for the application of Spd-CDs in enabling plants to contend against the challenges of global warming.

Conflicts of interest

The authors declare that they have no known competing financial interests or personal relationships that could have appeared to influence the work reported in this study.

Acknowledgements

References

1 H. Leridon, World population outlook: explosion or implosion?, *Popul. Soc.*, 2020, **573**(1), 1–4.

2 A. N. Wilson, M. J. Grieshop, J. Roback, S. Dell'Orco, J. Huang and J. A. Perkins, *et al.*, Efficacy, economics, and sustainability of bio-based insecticides from thermochemical biorefineries, *Green Chem.*, 2021, **23**, 10145–10156.

3 A. Soltani, S. M. Weraduwage, T. D. Sharkey and D. B. Lowry, Elevated temperatures cause loss of seed set in common bean (Phaseolus vulgaris L.) potentially through the disruption of source-sink relationships, *BMC Genomics*, 2019, **20**, 1–18.

4 R. R. M. Paterson, Longitudinal trends of future suitable climate for conserving oil palm indicates refuges in tropical south-east Asia with comparisons to Africa and South America, *Pac. Conserv. Biol.*, 2021, **28**, 57–67.

5 M. A. Gururani, J. Venkatesh and L. S. P. Tran, Regulation of photosynthesis during abiotic stress-induced photoinhibition, *Mol. Plant*, 2015, **8**, 1304–1320.

6 S. Sachdev, S. A. Ansari, M. I. Ansari, M. Fujita and M. Hasanuzzaman, Abiotic stress and reactive oxygen species: Generation, signaling, and defense mechanisms, *Antioxidants*, 2021, **10**, 277.

7 A. Bi, T. Wang, G. Wang, L. Zhang, M. Wassie and M. Amee, *et al.*, Stress memory gene FaHSP17.8-CII controls thermotolerance via remodeling PSII and ROS signaling in tall fescue, *Plant Physiol.*, 2021, **187**, 1163–1176.

8 M. Zaffagnini, S. Fermani, C. H. Marchand, A. Costa, F. Sparla and N. Rouhier, *et al.*, Redox homeostasis in photosynthetic organisms: novel and established thiol-based molecular mechanisms, *Antioxid. Redox Signaling*, 2019, **31**, 155–210.

608 | *Environ. Sci.: Nano*, 2023, **10**, 595–610

This journal is © The Royal Society of Chemistry 2023

9 M. Hasanuzzaman, M. B. Bhuyan, F. Zulfiqar, A. Raza, S. M. Mohsin and J. A. Mahmud, et al., Reactive oxygen species and antioxidant defense in plants under abiotic stress: Revisiting the crucial role of a universal defense regulator, *Antioxidants*, 2020, **9**, 681.

10 G. V. Lowry, A. Avellan and L. M. Gilbertson, Opportunities and challenges for nanotechnology in the agri-tech revolution, *Nat. Nanotechnol.*, 2019, **14**, 517–522.

11 M. A. Farooq, F. Hannan, F. Islam, A. Ayyaz, N. Zhang and W. Chen, et al., The potential of nanomaterials for sustainable modern agriculture: present findings and future perspectives, *Environ. Sci.: Nano*, 2022, **9**, 1926–1951.

12 T. Hofmann, G. V. Lowry, S. Ghoshal, N. Tufenkji, D. Brambilla and J. R. Dutcher, et al., Technology readiness and overcoming barriers to sustainably implement nanotechnology-enabled plant agriculture, *Nat. Food*, 2020, **1**, 416–425.

13 C. O. Dimkpa, U. Singh, P. S. Bindraban, W. H. Elmer, J. L. Gardea-Torresdey and J. C. White, Zinc oxide nanoparticles alleviate drought-induced alterations in sorghum performance, nutrient acquisition, and grain fortification, *Sci. Total Environ.*, 2019, **688**, 926–934.

14 D. Li, W. Li, H. Zhang, X. Zhang, J. Zhuang and Y. Liu, et al., Far-red carbon dots as efficient light-harvesting agents for enhanced photosynthesis, *ACS Appl. Mater. Interfaces*, 2020, **12**, 21009–21019.

15 Y. Li, Z. Tang, Z. Pan, R. Wang, X. Wang and P. Zhao, et al., Calcium-mobilizing properties of Salvia miltiorrhiza-derived carbon dots confer enhanced environmental adaptability in plants, *ACS Nano*, 2022, **16**, 4357–4370.

16 R. Alcázar, A. M. Fortes and A. F. Tiburcio, Polyamines in plant biotechnology, food nutrition, and human health, *Front. Plant Sci.*, 2020, **11**, 120.

17 L. Sharma, M. Priya, N. Kaushal, K. Bhandhari, S. Chaudhary and O. P. Dhankher, et al., Plant growth-regulating molecules as thermoprotectants: functional relevance and prospects for improving heat tolerance in food crops, *J. Exp. Bot.*, 2020, **71**, 569–594.

18 Y. J. Li, S. G. Harroun, Y. C. Su, C. F. Huang, B. Unnikrishnan and H. J. Lin, et al., Synthesis of self-assembled spermidine-carbon quantum dots effective against multidrug-resistant bacteria, *Adv. Healthcare Mater.*, 2016, **5**, 2545–2554.

19 V. Ruggieri, R. Calafiore, C. Schettini, M. M. Rigano, F. Olivieri and L. Frusciante, et al., Exploiting genetic and genomic resources to enhance heat-tolerance in tomatoes, *Agronomy*, 2019, **9**, 22.

20 M. K. Hasan, C. Liu, F. Wang, G. J. Ahammed, J. Zhou and M.-X. Xu, et al., Glutathione-mediated regulation of nitric oxide, S-nitrosothiol and redox homeostasis confers cadmium tolerance by inducing transcription factors and stress response genes in tomato, *Chemosphere*, 2016, **161**, 536–545.

21 M. Zhong, R. Song, Y. Wang, S. Shu, J. Sun and S. R. Guo, TGase regulates salt stress tolerance through enhancing bound polyamines-mediated antioxidant enzymes activity in tomato, *Environ. Exp. Bot.*, 2020, **179**, 104191.

22 H. Thordal-Christensen, Z. Zhang, Y. Wei and D. B. Collinge, Subcellular localization of H_2O_2 in plants. H_2O_2 accumulation in papillae and hypersensitive response during the barley-powdery mildew interaction, *Plant J.*, 1997, **11**, 1187–1194.

23 C. Dunand, M. Crèvecoeur and C. Penel, Distribution of superoxide and hydrogen peroxide in Arabidopsis root and their influence on root development: possible interaction with peroxidases, *New Phytol.*, 2007, **174**, 332–341.

24 M. Zhong, Y. Wang, Y. Zhang, S. Shu, J. Sun and S. R. Guo, Overexpression of transglutaminase from cucumber in tobacco increases salt tolerance through regulation of photosynthesis, *Int. J. Mol. Sci.*, 2019, **20**, 894.

25 S. V. Caemmerer and G. D. Farquhar, Some relationships between the biochemistry of photosynthesis and the gas exchange of leaves, *Planta*, 1981, **153**, 376–387.

26 G. J. Ethier and N. J. Livingston, On the need to incorporate sensitivity to CO_2 transfer conductance into the Farquhar-von Caemmerer-Berry leaf photosynthesis model, *Plant, Cell Environ.*, 2004, **27**, 137–153.

27 D. A. Ward and A. J. Keys, A comparison between the coupled spectrophotometric and uncoupled radiometric assays for RuBP carboxylase, *Photosynth. Res.*, 1989, **22**, 167–171.

28 R. Scheibe, K. Fickenscher and A. R. Ashton, Studies on the mechanism of the reductive activation of NADP-malate dehydrogenase by thioredoxin m and low-molecular-weight thiols, *Biochim. Biophys. Acta, Protein Struct. Mol. Enzymol.*, 1986, **870**, 191–197.

29 M. Zhong, Y. Wang, K. Hou, S. Shu, J. Sun and S. R. Guo, TGase positively regulates photosynthesis via activation of Calvin cycle enzymes in tomato, *Hortic. Res.*, 2019, **6**, 92.

30 Y. Nakano and K. Asada, Hydrogen peroxide is scavenged by ascorbate-specific peroxidase in spinach chloroplasts, *Plant Cell Physiol.*, 1981, **22**, 867–880.

31 K. J. Livak and T. D. Schmittgen, Analysis of relative gene expression data using real-time quantitative PCR and the $2^{-\Delta\Delta CT}$ method, *Methods*, 2001, **25**, 402–408.

32 J.-H. Chen, M. Tang, X.-Q. Jin, H. Li, L.-S. Chen and Q.-L. Wang, et al., Regulation of Calvin-Benson cycle enzymes under high temperature stress, *aBIOTECH*, 2022, 1–13.

33 S. Hussain, Z. Ulhassan, M. Brestic, M. Zivcak, W. Zhou and S. I. Allakhverdiev, et al., Photosynthesis research under climate change, *Photosynth. Res.*, 2021, **150**, 5–19.

34 M. L. Pérez-Bueno, M. Pineda and M. Barón, Phenotyping plant responses to biotic stress by chlorophyll fluorescence imaging, *Front. Plant Sci.*, 2019, **10**, 1135.

35 Y. Li, X. Xu, B. Lei, J. Zhuang, X. Zhang and C. Hu, et al., Magnesium-nitrogen co-doped carbon dots enhance plant growth through multifunctional regulation in photosynthesis, *Chem. Eng. J.*, 2021, **422**, 130114.

36 E. Kou, Y. Yao, X. Yang, S. Song, W. Li and Y. Kang, et al., Regulation mechanisms of carbon dots in the development of lettuce and tomato, *ACS Sustainable Chem. Eng.*, 2021, **9**, 944–953.

This journal is © The Royal Society of Chemistry 2023

Environ. Sci.: Nano, 2023, **10**, 595–610 | **609**

37 W. Li, S. Wu, H. Zhang, X. Zhang, J. Zhuang and C. Hu, et al., Enhanced biological photosynthetic efficiency using light-harvesting engineering with dual-emissive carbon dots, Adv. Funct. Mater., 2018, 28, 1804004.

38 Q. Chen, X. Cao, Y. Li, Q. Sun, L. Dai and J. Li, et al., Functional carbon nanodots improve soil quality and tomato tolerance in saline-alkali soils, Sci. Total Environ., 2022, 830, 154817.

39 M. Djanaguiraman, D. L. Boyle, R. Welti, S. V. K. Jagadish and P. V. V. Prasad, Decreased photosynthetic rate under high temperature in wheat is due to lipid desaturation, oxidation, acylation, and damage of organelles, BMC Plant Biol., 2018, 18, 1–17.

40 X. Yang, Y. Han, J. Hao, X. Qin, C. Liu and S. Fan, Exogenous spermidine enhances the photosynthesis and ultrastructure of lettuce seedlings under high-temperature stress, Sci. Hortic., 2022, 291, 110570.

41 D. Sugiura, E. Betsuyaku and I. Terashima, Interspecific differences in how sink–source imbalance causes photosynthetic downregulation among three legume species, Ann. Bot., 2019, 123, 715–726.

42 J.-H. Chen, S.-T. Chen, N.-Y. He, Q.-L. Wang, Y. Zhao and W. Gao, et al., Nuclear-encoded synthesis of the D1 subunit of photosystem II increases photosynthetic efficiency and crop yield, Nat. Plants, 2020, 6, 570–580.

43 Y. Takahashi, S. Wada, K. Noguchi, C. Miyake, A. Makino and Y. Suzuki, Photochemistry of photosystems II and I in rice plants grown under different N levels at normal and high temperature, Plant Cell Physiol., 2021, 62, 1121–1130.

44 P. Wang, Rewiring state transitions mediated by light-harvesting complex I, Plant Physiol., 2022, 188, 1936–1938.

45 H. M. Kalaji, A. Jajoo, A. Oukarroum, M. Brestic, M. Zivcak and I. A. Samborska, et al., Chlorophyll a fluorescence as a tool to monitor physiological status of plants under abiotic stress conditions, Acta Physiol. Plant., 2016, 38, 1–11.

46 Y. Qu, K. Sakoda, H. Fukayama, E. Kondo, Y. Suzuki and A. Makino, et al., Overexpression of both Rubisco and Rubisco activase rescues rice photosynthesis and biomass under heat stress, Plant Cell Environ., 2021, 44, 2308–2320.

47 G. E. Degen, D. J. Orr and E. C. Silva, Heat-induced changes in the abundance of wheat Rubisco activase isoforms, New Phytol., 2021, 229, 1298–1311.

48 M. Suganami, Y. Suzuki, Y. Tazoe, W. Yamori and A. Makino, Co-overproducing Rubisco and Rubisco activase enhances photosynthesis in the optimal temperature range in rice, Plant Physiol., 2021, 185, 108–119.

49 C. A. Raines, Improving plant productivity by re-tuning the regeneration of RuBP in the Calvin-Benson-Bassham cycle, New Phytol., 2022, 236, 350–356.

50 Y. Li, W. Li, X. Yang, Y. Kang, H. Zhang and Y. Liu, et al., Salvia miltiorrhiza-derived carbon dots as scavengers of reactive oxygen species for reducing oxidative damage of plants, ACS Appl. Nano Mater., 2020, 4, 113–120.

51 H.-I. Jung, M.-S. Kong, B.-R. Lee, T.-H. Kim, M.-J. Chae and E.-J. Lee, et al., Exogenous glutathione increases arsenic translocation into shoots and alleviates arsenic-induced oxidative stress by sustaining ascorbate-glutathione homeostasis in rice seedlings, Front. Plant Sci., 2019, 10, 1089.

52 Z. Hu, J. Li, S. Ding, F. Cheng, X. Li and Y. Jiang, et al., The protein kinase CPK28 phosphorylates ascorbate peroxidase and enhances thermotolerance in tomato, Plant Physiol., 2021, 186, 1302–1317.

53 N. Liu, J. Li, J. Lv, J. Yu, J. Xie and Y. Wu, et al., Melatonin alleviates imidacloprid phytotoxicity to cucumber (Cucumis sativus L.) through modulating redox homeostasis in plants and promoting its metabolism by enhancing glutathione dependent detoxification, Ecotoxicol. Environ. Saf., 2021, 217, 112248.

54 R. Mittler, S. I. Zandalinas, Y. Fichman and F. Van Breusegem, Reactive oxygen species signalling in plant stress responses, Nat. Rev. Mol. Cell Biol., 2022, 23, 663–679.

55 Y. Xu, Q. Xu and B. R. Huang, Ascorbic acid mitigation of water stress-inhibition of root growth in association with oxidative defense in tall fescue (Festuca arundinacea Schreb.), Front. Plant Sci., 2015, 6, 807.

56 F. A. Busch, J. Tominaga, M. Muroya, N. Shirakami, S. Takahashi and W. Yamori, et al., Overexpression of BUNDLE SHEATH DEFECTIVE 2 improves the efficiency of photosynthesis and growth in Arabidopsis, Plant J., 2020, 102, 129–137.

57 A. Paradiso, G. Domingo, E. Blanco, A. Buscaglia, S. Fortunato, M. Marsoni and P. Scarcia, et al., Cyclic AMP mediates heat stress response by the control of redox homeostasis and ubiquitin-proteasome system, Plant Cell Environ., 2020, 43, 2727–2742.

610 | Environ. Sci.: Nano, 2023, 10, 595–610

This journal is © The Royal Society of Chemistry 2023